ACS Energy LETTERS

http://pubs.acs.org/journal/aelccp

Letter

Enhanced PFAS Defluorination through Control of Radical-Dependent Degradation Pathways

Alexander Nitsche, Haldrian Iriawan,* Xiao Wang, Yuriy Román-Leshkov, and Yang Shao-Horn*

Cite This: https://doi.org/10.1021/acsenergylett.6c00597

Read Online

ACCESS | Metrics & More | Article Recommendations | Supporting Information

ABSTRACT: Per- and polyfluoroalkyl substances (PFAS) are persistent pollutants that are resistant to conventional water treatment. This study investigates the electrochemical degradation of perfluorooctanoic acid (PFOA) in perchlorate and sulfate electrolytes with boron-doped diamond. Quantification of PFOA degradation and fluoride (F^-) and short-chain perfluorocarboxylic acid (PFCA) formation showed similar defluorination efficiency in both electrolytes at 4.0 V_{RHE} but significantly higher PFCA yields with the sulfate electrolyte. Through electrochemistry-mass spectrometry, ^{19}F and ^{1}H NMR spectroscopy, potential-dependent investigation, and radical-scavenger experiments, we showed that both electrolytes exhibit similar decarboxylation rates of the carboxylic group to evolve CO_2. However, $HO^\bullet$ primarily drove C−F cleavage, releasing F^- and leaving the remaining fluorocarbon backbone hydrogenated, while $SO_4^{\bullet-}$ promoted C−C cleavage to form fully fluorinated shorter-chain PFCAs. These results highlight the distinct roles of free radicals in PFOA degradation, offering mechanistic insights to design electrolytes to promote complete PFAS defluorination and suppress the formation of short-chain PFAS.

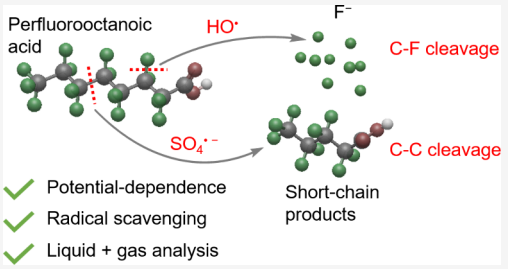

Per- and polyfluoroalkyl substances (PFAS) make up a class of synthetic chemicals that have been widely applied across industrial, commercial, and consumer products due to their exceptional chemical and thermal stability. Their use spans textiles, nonstick coatings, firefighting foams, and food packaging. However, the very properties that make PFAS useful, such as resistance to heat, acids, and biodegradation, also render them highly persistent in the environment.[1−3] As a consequence, PFAS have become pervasive pollutants, with widespread detection in surface and groundwater, soils, sediments, and even the blood serum of humans and wildlife.[4,5] Their bioaccumulation and persistence raise concerns regarding long-term health risks, including hormone disruption, developmental toxicity, as well as associations with certain cancers.[4,6]

Conventional water treatment methods such as adsorption and membrane filtration can remove PFAS from water but typically leave the chemical structure of the molecule intact.[7] Therefore, increasing efforts have been directed toward destructive techniques that aim not only to remove PFAS but also to mineralize them into harmless end products. One of the central challenges of this method is the cleavage of the exceptionally stable C−F bond (≈400 kJ mol^{-1}).[8] Thus, a wide range of degradation strategies have been explored, including electrochemical methods,[9−13] photochemical approaches,[14−16] sonolysis,[17,18] plasma-based techniques,[19] and other oxidative treatments.[20] A particularly promising strategy is electrochemical oxidation, which enables the generation of highly reactive oxidative species, such as free radicals, at the electrode−electrolyte interface.[21−26] Electrochemical degradation can be operated under ambient conditions, coupled with renewable electricity, and implemented in modular configurations compatible with existing water treatment infrastructure, enhancing its applicability for real-world PFAS-contaminated waters.[27−29] These advantages have positioned electrochemical oxidation as a leading candidate for PFAS degradation, motivating growing interest in radical-mediated degradation pathways at advanced anode materials.[9−13]

In enabling the electrochemical generation of free radicals, an inert electrode such as boron-doped diamond (BDD) is widely used for PFAS degradation. As a "non-active" anode, BDD is understood to promote the formation of weakly adsorbed hydroxyl radicals ($HO^\bullet$) from water,[30,31] which have been detected using radical scavengers like DMPO, based on the emergence of characteristic peaks in the magnetic field region of ∼ 3400 G using Electron Paramagnetic Spectroscopy. This signal matches the $HO^\bullet$ standard from the Fenton reaction ($H_2O_2 + Fe^{2+} \rightarrow HO^\bullet + OH^- + Fe^{3+}$).[32,33] The $HO^\bullet$ radicals can attack PFAS molecules, leading to their stepwise transformation into short-chain perfluorocarboxylic acids (PFCAs), fluoride ions (F^-), and CO_2.[34−36] In addition to $HO^\bullet$, other reactive species such as sulfate radicals ($SO_4^{\bullet-}$),

Received: February 25, 2026
Revised: March 30, 2026
Accepted: April 8, 2026

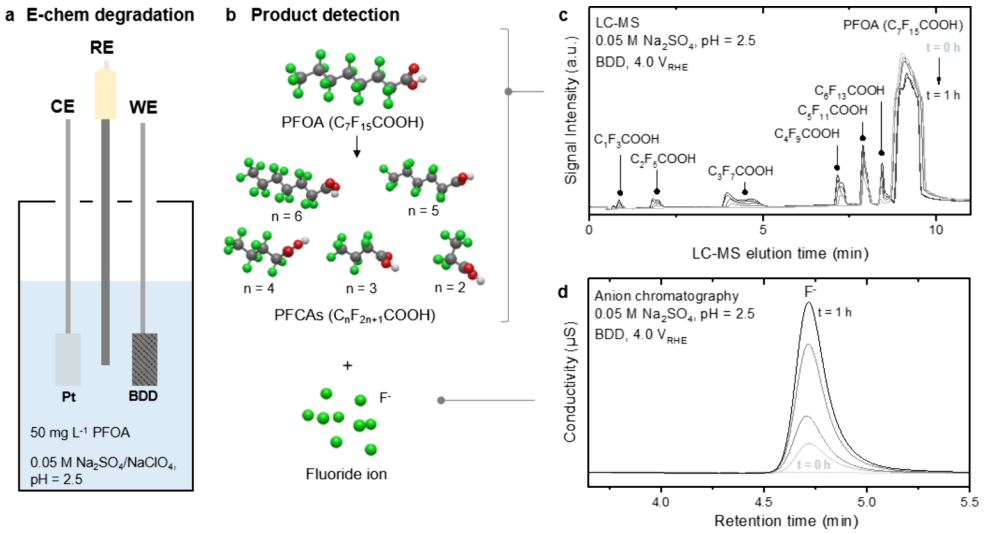

Figure 1. Electrochemical PFOA degradation in a single-compartment cell on a boron doped diamond (BDD) electrode at 4.0 V_{RHE}. (a) Schematic illustration of the setup used for PFOA degradation. (b) PFOA was degraded into short-chain PFCAs ($C_nF_{2n+1}COOH$, n = 1−6) and fluoride. (c) LC-MS spectra recorded at different reaction times (0, 15, 30, 45, 60 min) in sulfate (0.05 M Na_2SO_4, pH 2.5) electrolyte. The shading of the signal curves darkens progressively with an increasing electrolysis time. The signals can be assigned to PFOA and short-chain PFCAs.[44] (d) Anion chromatography spectra at different reaction times. Fluoride is detected at a retention time of ∼ 4.7 min.

singlet oxygen, and direct electron transfer processes can be generated depending on the electrolyte compositions, which has been shown to influence the degradation efficiency.[11] For PFOA, which is one of the most widely studied PFAS,[21] defluorination efficiency ranging from 15% to over 40% has been reported,[13,22−26] which is highly dependent on factors such as electrode material, applied potential or current density, electrode surface area, electrolyte composition, initial PFAS concentration, and pH (Table S1), rendering cross-study comparisons challenging.

Nevertheless, an understanding of the electrolyte dependence on PFOA degradation kinetics and speciation has emerged. First, acidic pH has been reported to enhance electrochemical PFOA degradation relative to neutral or alkaline conditions.[13,37,38] A possible explanation for the faster PFOA degradation is the higher concentration of $HO^•$ under acidic conditions,[37] which likely results from the longer lifetime of $HO^•$ in acidic compared to neutral pH.[39] For example, a study where $HO^•$ was generated via nonthermal plasma reported a ∼ 2.5 higher steady-state $HO^•$ concentration and lifetime at pH = 3 compared to pH = 7.[39] Moreover, CO_2 which is generated through electrochemical PFAS mineralization converts to HCO_3^-/CO_3^{2-} at neutral/alkaline pH, which scavenges $HO^•$ and suppresses $HO^•$-mediated degradation pathways.[40,41] Second, oxidizing species generated at the anode — governed by the electrolyte anions — strongly influence which bonds are attacked during PFOA degradation.[30] Previous studies[11,38] using BDD anodes in sulfate electrolytes have shown that $SO_4^{•-}$ radicals dominate the initiation step, oxidizing the carboxylate group via one-electron transfer to trigger Kolbe decarboxylation, CO_2 release, and formation of perfluoroalkyl radicals. This assumption is supported by radical-scavenging experiments and by enhanced degradation rates with increasing sulfate or persulfate concentration.[11,38] Meanwhile, $HO^•$ radicals are found to be less effective at initiating direct oxidation of intact PFOA but contribute to downstream oxidation of perfluoroalkyl radical intermediates, thereby facilitating stepwise chain shortening and defluorination.[11] While in these studies the PFOA decay is monitored under the impact of radical scavengers or under different reaction conditions,[11,38] it is not investigated whether the observed decay results from an actual breakdown of PFOA into shorter perfluorinated chains or from defluorination, leaving the carbon backbone intact. Another body of work challenges the notion of higher reactivity of $SO_4^{•-}$ toward PFAS degradation and instead poses $HO^•$ to be the more effective oxidant. For example, a study[36] uses UV irradiation to form $HO^•$ and $SO_4^{•-}$ radicals from H_2O_2 and $S_2O_8^{2-}$ precursors, respectively, allowing the role of the two radicals to be studied independently from each other. This work shows — in agreement with other reports[42,43] — higher reaction rate constants with perfluorinated compounds (e.g., trifluoroacetate, perfluoropropionic acid, perfluorobutyric acid) for $HO^•$ than for $SO_4^{•-}$ radicals. This is in contradiction to the studies discussed before,[11,38] which report faster PFOA degradation with $SO_4^{•-}$ radicals. In summary, the distinct mechanistic roles of free radicals, particularly $HO^•$ and $SO_4^{•-}$, during PFOA degradation remain unclear in light of the conflicting evidence.[11,36,38] A systematic investigation is needed to disentangle the roles of $HO^•$ and $SO_4^{•-}$ radicals in PFOA degradation and the tendency for F^- versus PFCA formation to inform future electrolyte designs for more efficient PFAS degradation.

This study examines the electrochemical degradation of perfluorooctanoic acid (PFOA) in perchlorate and sulfate electrolytes by using a boron-doped diamond (BDD) anode. Acidic pH (2.5) is chosen to ensure higher steady-state concentrations of $HO^•$ radicals and minimize the scavenging effect of dissolved CO_2 as bicarbonate, which would render the efficacy of $HO^•$ ambiguous. Quantification of PFOA removal, fluoride (F^-) release, and short-chain perfluorocarboxylic acid (PFCA) formation revealed comparable rates of PFOA removal and F^- release in both electrolytes at 4.0 V_{RHE}, whereas substantially higher PFCA yields were observed in the sulfate system. Furthermore, electrochemistry-mass spectrometry (EC-MS) showed a similar CO_2 evolution in both electrolytes, indicating comparable rates of decarboxylation of the carboxyl group. Postelectrolysis NMR analysis revealed the

https://doi.org/10.1021/acsenergylett.6c00597
ACS Energy Lett. XXXX, XXX, XXX−XXX

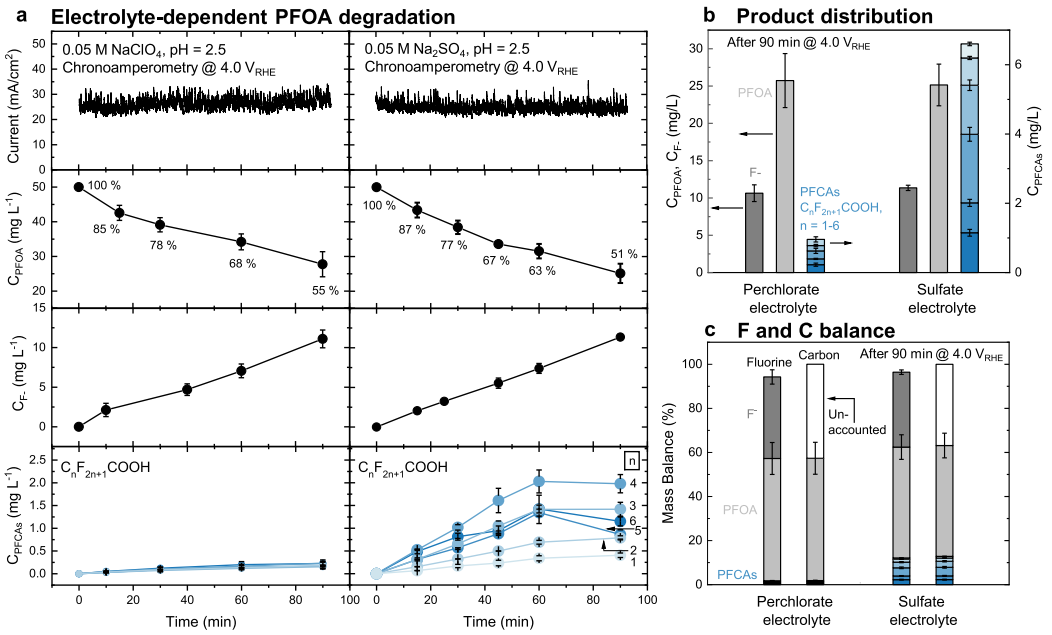

Figure 2. Electrolyte-dependent PFOA degradation in perchlorate and sulfate electrolyte at a constant potential of 4.0 V_{RHE}. The error bars represent the standard deviation (n = 3). (a) Current profile, PFOA concentration, fluoride concentration, and short-chain PFCA concentration for perchlorate (left panels) and sulfate (right panels) electrolyte during 90 min electrolysis. (b) Concentration of PFOA, fluoride, and PFCAs after 90 min electrolysis. (c) Fluorine and carbon mass balance after 90 min electrolysis; see Supporting Information for calculation. The white bar in the carbon mass balance shows the unaccounted difference to 100%.

formation of partially hydrogenated fluorocarbon species in perchlorate electrolyte and short-chain PFCAs in sulfate electrolyte. Finally, potential-dependent experiments and radical scavenging tests using *tert*-butanol as hydroxyl radical ($HO^{\bullet}$) scavenger demonstrated that $HO^{\bullet}$ is primarily responsible for C−F bond cleavage leading to F^- formation and hydrogenation of the carbon backbone, while sulfate radicals ($SO_4^{\bullet-}$) preferentially induce C−C bond scission along the perfluoroalkyl chain, generating fully fluorinated short-chain PFCAs. Together, these findings elucidate the distinct roles of reactive radicals in PFOA degradation and provide mechanistic guidance in the design of electrolytes for more efficient PFAS treatment.

IMPACT OF ELECTROLYTES ON PERFLUOROOCTANOIC ACID (PFOA) DEGRADATION: PERCHLORATE VS SULFATE ELECTROLYTE

PFOA degradation was carried out in a single compartment cell with a commercial boron-doped diamond (BDD) electrode on a niobium substrate as working electrode (Figure 1a, see Supporting Information for experimental details), where short-chain PFCAs and F^- ions were detected via liquid-chromatography mass spectrometry (LC-MS) and anion chromatography, respectively, with a focus to close the F mass balance (Figure 1b-d and Figure S1, S2). The degradation experiments of PFOA with a starting concentration of 50 mg L^{-1} were performed by holding the working electrode potential at 4.0 V_{RHE} (Figure S3) in 0.05 M $NaClO_4$ (perchlorate) or 0.05 M Na_2SO_4 (sulfate) electrolytes at pH 2.5 as a function of the degradation time. LC-MS spectra of the PFOA-containing electrolyte collected during degradation showed decreasing PFOA peak intensities and the emergence of several new peaks, which can be assigned to short-chain perfluorocarboxylic acids (PFCAs, $C_nF_{2n+1}COOH$, n = 1−6) from PFOA degradation (Figure 1c).[12,44,45] Meanwhile, the fluoride concentration increased linearly over the degradation time, as indicated by the increasing F^- peak in the anion chromatogram (Figure 1d). This protocol enables the measurement of PFOA degradation and the associated product distribution (i.e., F^- versus short-chain PFCA formation), which will be compared across the two electrolytes.

Both the perchlorate and sulfate electrolytes showed comparable reduction of the PFOA signal and formation of F^- but more PFCAs with fluorinated short chains in the case of the sulfate electrolyte. Upon the constant potential measurement at 4.0 V_{RHE} with *iR*-correction, where a steady-state current of ∼ 25 mA cm^{-2} was measured for both electrolytes (Figure 2a, top panel), the PFOA concentration decreased from 50 to 28 ± 3.6 and 26 ± 2.8 mg L^{-1} for the perchlorate and sulfate electrolytes, respectively (Figure 2a, second row), following first-order kinetics (Figure S4). While this apparent first-order behavior is consistent with prior studies,[11] it may originate from reaction kinetics or mass transport (see Supporting Information). The fluoride concentration increased almost linearly over time, with a slope of ∼ 0.13 ppm min^{-1} for both electrolytes (Figure 2a, third row), indicating nearly identical F^- formation rates. Accordingly, the defluorination efficiency, calculated via the ratio of F^- concentration by the total fluorine concentration in the electrolyte (see Supporting Information for calculation details) increased linearly with time to ∼ 35% over 90 min for both electrolytes (Figure S5). Despite the similarities in the PFOA reduction and the degree of defluorination, significant differences were observed in the concentrations of short-chain PFCAs over time (Figure 2a, bottom panel) in these two electrolytes. The PFCA concentration associated with perchlorate remained negligible (<0.3 mg L^{-1} in total) while that in the sulfate electrolyte was

https://doi.org/10.1021/acsenergylett.6c00597
ACS Energy Lett. XXXX, XXX, XXX−XXX

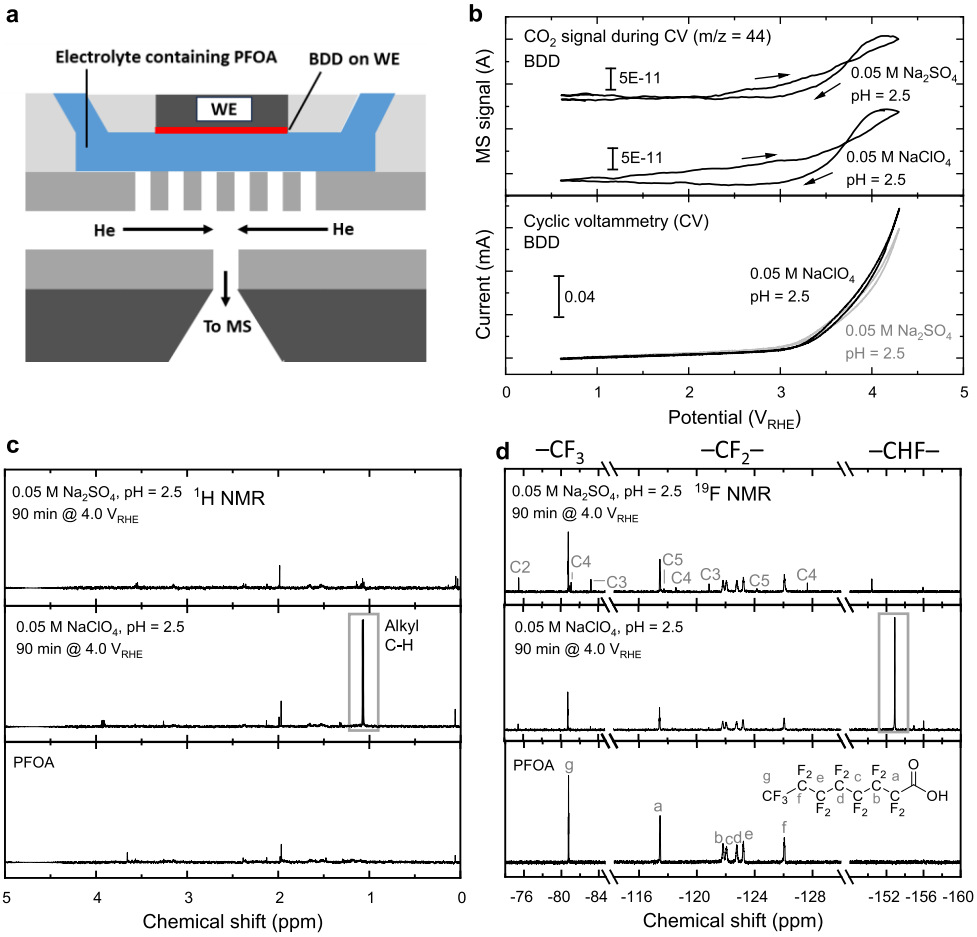

Figure 3. Electrochemical mass spectrometry (EC-MS) and NMR analyses of PFOA degradation on BDD. (a) Schematic illustration of the EC-MS setup used to monitor gaseous products formed during PFOA degradation (modified from ref.[44]). (b) CO_2 (m/z 44) signal (upper panel) recorded during cyclic voltammetry (CV) (lower panel) at a scan rate 20 mV s^{-1} in perchlorate and sulfate electrolyte, respectively. (c, d) Postelectrolysis ^1H and ^{19}F NMR spectra in perchlorate and sulfate electrolyte, and PFOA reference measurement, respectively. In (d), three signal regions corresponding to $-CF_3$, $-CF_2$-, and −CHF- are shown; signals were assigned based on published ^{19}F NMR reference spectra (ref.[49,50]). In the upper panel of (d), signals corresponding to short-chain PFCAs are shown; e.g., C5 corresponds to C_4F_9COOH.

significant (6.5 mg L^{-1} in total) after 90 min, as shown in Figure 2b. The concentration of PFCAs increased steadily up to 60 min and then stagnated or decreased between 60 and 90 min in the sulfate electrolyte despite continued PFOA decay and F^- formation. Among PFCAs, the intermediate length n = 4 (C_4F_9COOH) had the highest concentration (2.0 mg L^{-1}, also across the 90 min period) compared to the longer-chain (n = 6, 1.2 mg L^{-1}) and shorter-chain (<1.0 mg L^{-1} for n = 1, 2) PFCAs. This observation may indicate the conversion of serially longer-chained to shorter-chained PFCAs. An extended electrolysis experiment up to 3 h in sulfate electrolyte confirmed continued PFOA degradation following first-order kinetics, while the F^- concentration and the defluorination ratio are increasing linearly (Figure S6). In contrast, the concentration of short-chain PFCAs plateaued after the initial increase. This behavior suggests that a steady state is reached in which short-chain PFCA formation from PFOA is balanced by its further degradation through sequential chain shortening, decarboxylation, and defluorination pathways. This steady-state interpretation is supported by the observation that the concentration of PFCAs in the electrolyte is in a similar range compared to PFOA concentration when the plateau in PFCA concentration after ∼ 60 min electrolysis is reached (Figure S7).

A comprehensive assessment of reaction product speciation was performed through the analysis of the carbon and fluorine mass balance. A fluorine mass balance after 90 min was calculated for both electrolytes (Figure 2c, mass balance over time in Figure S8). The fluorine mass balance was determined by dividing the molar concentration of fluorine detected in the postelectrolysis electrolyte, which consisted of F^-, PFCAs, and unreacted PFOA, each normalized with their respective number of fluorine atoms, by the initial fluorine concentration (see Supporting Information for detailed calculation). For both electrolytes, the fluorine mass balance was closed within experimental certainty, indicating that there were no other fluorine-containing species in the electrolyte that were not detected. In addition, a carbon mass balance was determined (Figure 2c) by dividing the molar concentrations of perfluorocarboxylic acids and unreacted PFOA detected in the postelectrolysis electrolyte, normalized with their respective number of carbon atoms, by the initial concentration of PFOA (see Supporting Information for detailed calculation). The carbon mass balance was not closed as the remaining PFOA and PFCAs after 90 min of electrolysis only added up to 59% and 65% of the initial value for the perchlorate and sulfate electrolytes, respectively. The unaccounted difference to 100% is indicated by a white bar. The fact that the mass balance is

https://doi.org/10.1021/acsenergylett.6c00597
ACS Energy Lett. XXXX, XXX, XXX−XXX

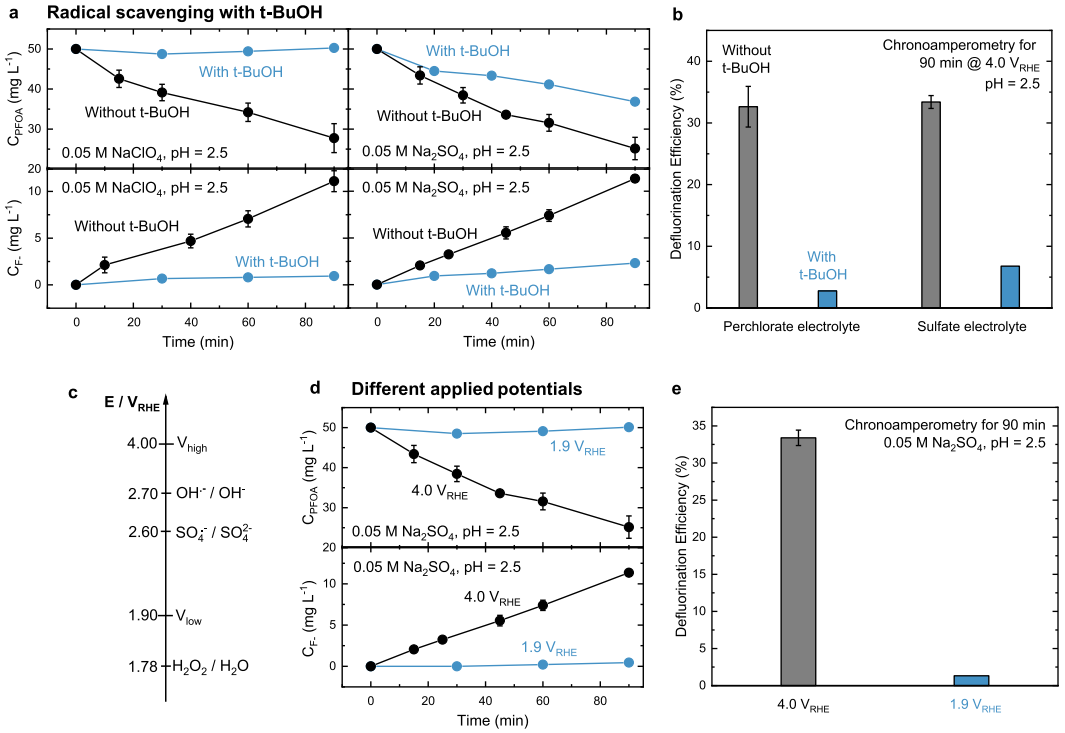

Figure 4. Identification of reactive species governing PFOA degradation in perchlorate and sulfate electrolytes. The error bars represent the standard deviation (n = 3). (a) Concentration profile of PFOA and fluoride over time in perchlorate (left) and sulfate (right) electrolytes, with and without the presence of *tert*-butanol (*t*-BuOH) as the $HO^{\bullet}$ scavenger. (b) Defluorination efficiency after 90 min electrolysis at 4 V_{RHE}, with and without *t*-BuOH. (c) Standard oxidation potentials of hydroxyl radicals, sulfate radicals, and H_2O_2 are compared to the potentials of 4.0 V_{RHE} (V_{high}) and 1.9 V_{RHE} (V_{low}), at which PFOA degradation was examined. (d) Concentration of PFOA and fluoride during electrolysis at 4.0 V_{RHE} and 1.9 V_{RHE} in sulfate electrolyte. (e) Defluorination efficiency after 90 min of electrolysis in sulfate electrolyte at 4.0 V_{RHE} and 1.9 V_{RHE}, respectively.

closed for fluoride but not for carbon can be attributed to the generation of carbon-containing gas products like the mineralization of PFOA to CO_2,[10,25,46−48] which will be examined further via electrochemical-mass spectrometry in the next section. Overall, these results highlight the higher tendency for the formation of short-chain PFCAs in the sulfate electrolyte despite the nearly identical PFOA degradation and degree of defluorination (Figure S5) reached in the two electrolytes.

REACTION PRODUCT CHARACTERIZATION AND MECHANISTIC IMPLICATIONS THROUGH EC-MS AND ^{19}F NMR

Detection of CO_2 via EC-MS sheds light into the unclosed carbon balance (Figure 2c) and points to decarboxylation of the −COOH group as the origin of CO_2 release. Cyclic voltammetry (CV) was performed between 0.9 and ∼ 4.0 V_{RHE} in perchlorate and sulfate electrolyte while simultaneously detecting reaction products by mass spectrometry (Figure 3a,b). The onset potential, defined here as the potential at which the current reached 5% of the maximum current, was 2.9 V_{RHE} for both electrolytes. In the case of both electrolytes, CO_2 (m/z 44 and its fragment at m/z 28) and O_2 (m/z 32, Figure S9) were detected. We attribute the O_2 signal to the oxygen evolution reaction (OER) at the anode. The CO_2 signal can be assigned to PFOA degradation, as PFOA was the only carbon-containing species in solution. The comparable CO_2 evolution in both electrolytes (Figure 3b) suggests that CO_2 formation originates from a pathway largely insensitive to the electrolyte anion. We attribute the CO_2 evolution to decarboxylation of the − COOH functional group of PFOA, proceeding similarly in both perchlorate and sulfate electrolytes via the Kolbe-like reaction $C_nF^{\bullet}_{2n+1}COOH \rightarrow C_nF^{\bullet}_{2n+1} + CO_2 + H^+ + e^-$, once radical generation is initiated at elevated potentials.[22,47] To support this hypothesis, we further analyzed the carbon mass balance, where the unaccounted fraction (0.42 in perchlorate and 0.37 in sulfate electrolyte, Figure 2c) could be assigned to CO_2, in light of the gas analysis from EC-MS. In order to assess how much the evolved CO_2 can be attributed to the decarboxylation of the carboxylic acid groups versus the oxidation of the fluorinated carbon backbone, a COOH balance analysis has been conducted. Mathematically, the calculation is shown via eq 1, where the moles of evolved CO_2 ($n_{CO2\ evolved}$), approximated by the initial PFOA concentration multiplied by the unaccounted fraction in the carbon balance, was divided by the moles of the carboxylic acid group consumed ($n_{COOH\ consumed}$), which is obtained by subtracting the concentration of PFCAs from the concentration of consumed PFOA since each PFOA and PFCA molecule possesses one carboxylic acid group. For both electrolytes, the ratio was close to 1 within experimental uncertainty (1.03 and 1.21 for perchlorate and sulfate electrolytes, respectively; see Supporting Information for detailed calculation), indicating that the evolved CO_2 almost exclusively stems from decarboxylation of the carboxylic groups in PFOA and PFCAs, while the carbon backbone likely remains as solution-phase products.

https://doi.org/10.1021/acsenergylett.6c00597
ACS Energy Lett. XXXX, XXX, XXX−XXX

$$R_{CO_2 from-COOH} = \frac{n_{CO2evolved}}{n_{COOHconsumed}} \approx \frac{c_{PFOA,unaccounted}}{c_{PFOA,consumed} - c_{PFCA,produced}} = \frac{x_{unaccounted} \cdot \text{Initial PFOA concentration}\left(\frac{mmol}{L}\right)}{c_{PFOA,consumed}\left(\frac{mmol}{L}\right) - c_{PFCA,produced}\left(\frac{mmol}{L}\right)} \quad (1)$$

^{19}F and ^{1}H NMR showed the formation of an H-terminated carbon backbone in perchlorate electrolyte and short-chain PFCAs in sulfate electrolyte, providing further support for the discussed differences in the degradation pathways. In post-electrolysis ^{19}F NMR spectra in the sulfate electrolyte (Figure 3c,d), characteristic resonances of short-chain PFCAs were detected, while the perchlorate electrolyte showed no detectable PFCA signals, in line with previous interpretations (Figure 2). Instead, in the case of perchlorate electrolyte, a strong ^{19}F resonance in the −CHF- region and corresponding alkyl proton signals in the ^{1}H NMR spectra indicate partial hydrogenation of the carbon backbone following defluorination, while the carbon backbone largely remained intact. These observations indicate C−F bond cleavage followed by hydrogen termination in perchlorate electrolyte, whereas sulfate electrolyte promotes C−C scission leading to short-chain PFCAs. To elucidate this difference, we next systematically investigated the electrolyte-dependent active species (i.e., free radicals) in the two electrolytes via radical-scavenging and potential-dependent experiments.

IDENTIFYING ACTIVE SPECIES DRIVING PFOA DEGRADATION

In the two electrolytes, there is a significant difference in the amount of short-chain PFCAs formed through PFOA degradation (Figure 2b), indicating electrolyte-dependent tendencies for C−F bond cleavage, which yields fluoride, and C−C bond cleavage, which produces short-chain PFCAs. As a "non-active anode", BDD electrodes have been reported to facilitate the generation of $HO^{\bullet}$ at ∼ 2.70 V_{RHE}, which could act as oxidants during electrochemical oxidation processes.[30,31,51] $HO^{\bullet}$ can be formed through direct oxidation of water at the BDD surface (eq 2), experimentally shown via EPR spin-trapping.[30,31]

$$BDD + H_2O \rightarrow BDD(HO^{\bullet}) + H^+ + e^- \quad (2)$$

Additionally, in sulfate-containing electrolytes, BDD can also generate sulfate radicals ($SO_4^{\bullet-}$) via multiple pathways:[30,31] (i) direct electro-oxidation of sulfate anions on the BDD surface (eq 3), (ii) oxidation of sulfate by electrogenerated hydroxyl radicals (eq 4), and (iii) activation of persulfate ($S_2O_8^{-2}$) that can be formed in situ from sulfate (eq 5−6). The oxidation potential of sulfate radicals is ∼ 2.60 V_{RHE} at pH 2.5 (Figure 4c).[30,31,51] Thus, in sulfate electrolyte, both $HO^{\bullet}$ and $SO_4^{\bullet-}$ radicals can be generated by BDD, whereas in perchlorate electrolyte (where the anion is inert) only $HO^{\bullet}$ is present.

$$SO_4^{2-} \rightarrow SO_4^{\bullet-} + e^- \quad (3)$$

$$SO_4^{2-} + HO^{\bullet} \rightarrow SO_4^{\bullet-} + OH^- \quad (4)$$

$$2SO_4^{2-} \rightarrow S_2O_8^{2-} + 2e^- \quad (5)$$

$$S_2O_8^{2-} + e^- \rightarrow SO_4^{\bullet-} + SO_4^{2-} \quad (6)$$

To disentangle the contribution of $HO^{\bullet}$ and $SO_4^{\bullet-}$ during PFOA degradation, tert-butanol (*t*-BuOH) was used as a selective $HO^{\bullet}$ scavenger (100 mM) because its reaction rate constant with $HO^{\bullet}$ ($k \approx 6 \times 10^8$ M^{-1} s^{-1}) is ∼ 3 orders of magnitude higher than with $SO_4^{\bullet-}$ ($k \approx 10^5$ M^{-1} s^{-1}).[11,36] Therefore, the addition of *t*-BuOH effectively suppresses $HO^{\bullet}$-driven pathways while largely preserving the $SO_4^{\bullet-}$ reactivity, enabling discrimination between the roles of the two radicals.

In the perchlorate electrolyte (Figure 4a, left), in the presence of *t*-BuOH (light blue traces), no PFOA degradation and F^- formation was detected. These results demonstrate that $HO^{\bullet}$ is the key species driving C−F bond cleavage in PFOA degradation and that the suppression of $HO^{\bullet}$ formation effectively halts this pathway. In the sulfate electrolyte, in the presence of *t*-BuOH, the rate of PFOA degradation decreased (26% degradation after 90 min compared to 48% without *t*-BuOH, Figure 4a, right) but was still measurable compared to the perchlorate case, which suggests that $SO_4^{\bullet-}$ can break down PFOA into smaller components albeit less effectively than without *t*-BuOH. Meanwhile, F^- formation was suppressed to ∼ 0.02 ppm min^{-1} (from ∼ 0.13 ppm min^{-1} without *t*-BuOH) while short-chain PFCAs were detected in the presence of *t*-BuOH (Figure S10), however, with reduced concentrations compared to the case without *t*-BuOH; e.g., the concentration of C_4F_9COOH after 90 min was 0.9 mg L^{-1}, compared to 2.0 mg L^{-1} without *t*-BuOH. The reduced efficiency of $SO_4^{\bullet-}$ in forming short-chain PFCAs in the presence of *t*-BuOH can be attributed to two factors: (i) *t*-BuOH, which strongly scavenges $HO^{\bullet}$, also reacts weakly with $SO_4^{\bullet-}$ ($k \approx 10^5$ M^{-1} s^{-1}) and, thereby, reduces its activity; and (ii) the generation of $SO_4^{\bullet-}$ partly relies on $HO^{\bullet}$ via eq 4, so scavenging $HO^{\bullet}$ indirectly decreases the concentration of $SO_4^{\bullet-}$. To further verify the role of the electrolyte anion, PFOA degradation was performed by using sodium nitrate ($NaNO_3$) as the supporting electrolyte (Figure S11, 0.05 M $NaNO_3$, pH 2.5, otherwise identical conditions as in Figure 2a), where the inert anion would not further oxidize and generate additional species beyond $HO^{\bullet}$. The degradation behavior closely mirrored that observed in the perchlorate electrolyte, where nearly identical PFOA decrease and F^- formation was observed, with only trace amounts of short-chain PFCAs detected (Figure S11). The nearly identical degradation behavior observed in perchlorate and nitrate electrolytes indicates that the electrolyte anions remained electrochemically inert under the applied conditions, supporting the notion that no additional reactive species beyond $HO^{\bullet}$ are generated and that electrolyte decomposition does not contribute measurably to the observed PFOA degradation. Overall, these results demonstrate that hydroxyl radicals are primarily responsible for C−F bond cleavage, leading to fluoride release, while sulfate radicals which are present only in the sulfate electrolyte promote the fragmentation of PFOA to short-chain PFCAs.

To further support the idea that the free radicals are responsible for the observed degradation phenomena, PFOA electrolysis was performed at a reduced potential of 1.9 V_{RHE}, which lies below the oxidation potentials required for the formation of hydroxyl and sulfate radicals (Figure 4c). The concentration profiles of PFOA and fluoride over time for working potentials of 4.0 and 1.9 V_{RHE} are compared (Figure 4d). As previously discussed, electrolysis at 4.0 V_{RHE} resulted in a steady decrease in the PFOA concentration accompanied by a continuous increase in fluoride concentration, reflecting efficient C−F bond cleavage and progressive defluorination. In

https://doi.org/10.1021/acsenergylett.6c00597
ACS Energy Lett. XXXX, XXX, XXX−XXX

stark contrast, at 1.9 V_{RHE} the PFOA concentration remained essentially constant throughout the experiment, and only minor fluoride release was detected. The pronounced potential dependence is further illustrated when comparing the defluorination efficiencies after 90 min of electrolysis (35% defluorination at 4.0 V_{RHE}, compared to ~ 1% at 1.9 V_{RHE}, Figure 4e). Moreover, the possible involvement of H_2O_2 as an active species was examined (Figure S12),[20] using titanium oxysulfate ($TiOSO_4$) as a colorimetric reagent for H_2O_2.[52] In the absence of PFOA at 4.0 V_{RHE}, no H_2O_2 was generated on BDD, which eliminated the possible H_2O_2 contribution to PFOA degradation. These results clearly demonstrate that potentials below the radical generation threshold are insufficient to drive PFOA degradation.

ESTIMATION OF FARADAIC EFFICIENCY AND ENERGY CONSUMPTION

Through these mechanistic insights of the possible electron transfer events during bond-breaking of PFAS degradation, we estimate the faradaic efficiency (FE) of PFOA degradation with BDD and the associated electrical energy demand in the case of the perchlorate electrolyte (see Supplementary Note 1 for detailed calculations). We consider two scenarios of charge accounting during PFOA degradation: 1) complete PFOA mineralization to CO_2 as the terminal oxidized carbon product, and 2) PFOA oxidation to the reaction products detected in this work, i.e., CO_2, F^-, short-chain PFCAs, and alkyl/hydrogenated carbon backbone. In scenario 1, where all of the carbon in PFOA is oxidized to CO_2 via $14H_2O + C_7F_{15}COOH \rightarrow 8\ CO_2 + 29\ H^+ + 15\ F^- + 14\ e^-$, the maximum FE toward CO_2 achieved through complete PFOA mineralization is small because only micromoles of PFOA are present in the electrolyte, yielding an upper bound of 2.4% FE for CO_2. In scenario 2, the FE is an additive sum associated with four electrochemical events: CO_2 production from the −COOH decarboxylation, C−F bond cleavage to liberate F^-, C−C cleavage to generate short-chain PFCAs, and hydrogenation of the defluorinated carbon backbone. First, consistent with the COOH balance and EC-MS results, the observed CO_2 evolution is dominated by decarboxylation via $C_7F_{15}COOH \rightarrow C_7F_{15}^{\bullet} + CO_2 + H^+ + e^-$. Estimating one electron per CO_2 in a Kolbe-like step[22] gives an FE for CO_2 of ~ 0.03%. Furthermore, the defluorination observed experimentally corresponds to an FE of 0.86%, under a one-electron-per-F^- estimate (Scheme 1). With regard to C−C cleavage, short-chain PFCA formation in perchlorate electrolyte was negligible (0.003% FE) assuming that one electron transfer is required per C−C bond (Scheme 1). Finally, accounting for subsequent hydrogen termination of the defluorinated backbone (estimated here as three electrons per hydrogenation event) yields an FE of 2.6%. Summing up the four contributions measured experimentally shows that only ~ 3−4% of the charge is associated with PFAS-relevant conversion steps in case of the perchlorate electrolyte, implying that parasitic reactions — most notably oxygen evolution reaction — dominate the current under these conditions. Prior electrochemical PFAS studies often operate at substantially higher total currents while achieving comparable removal rates (Table S1), indicating that the FEs toward PFAS-relevant pathways are likely even lower. Using a cell voltage approximated by the applied anode potential (4.0 V_{RHE}) and neglecting additional ohmic losses, the electrical energy input was estimated as 7.5 kWh m^{-3}, corresponding to an energy of 29.8 kWh m^{-3} $order^{-1}$ to reduce the PFOA concentration by 1 order of magnitude. These values fall within the lower range reported for electrochemical PFAS treatment (1−100 kWh m^{-3}, ref.[53]). Note that the energy estimates in this study, based only on the applied anode potential, are lower bounds because real operation requires the full cell voltage, which includes cathodic overpotential and ohmic (iR) losses in the electrolyte. Since the energy-per-order scales with the cell voltage (see Supporting Information), using an anode-only proxy (e.g., ~ 4 V) can substantially understate energy relative to practical BDD operation, where the cell voltage is commonly ~ 12−20 V (e.g., ~ 16−20 V at ~ 40 mA cm^{-2}),[54] leading to an underestimation on the order of ~ 3−5. In addition, auxiliary energy demands (e.g., electrolyte pumping) are not captured in this estimate. Therefore, although the present results indicate favorable intrinsic energy metrics under idealized conditions, further improvements in anodic selectivity (i.e., suppression of the OER while sustaining radical formation) and overall system efficiency will be required to establish practical and energy-efficient PFAS treatment processes. Moreover, significant challenges related to scalability remain, including the high cost of large boron-doped diamond electrode surface areas, complex reactor designs, limitations in mass transport at high flow rates, and electrode fouling.[53] A comprehensive technoeconomic analysis will therefore be essential to assess the viability of electrochemical PFAS treatment and to identify the key performance metrics (e.g., faradaic efficiency, current density, electrode lifetime, and system energy efficiency) required to enable economically feasible operation. A simple throughput estimate (see Supporting Information) indicates that, based on the observed faradaic efficiencies, intrinsic PFAS degradation rates could, in principle, reach ~ 1−10 kg m^{-2} day^{-1} under idealized assumptions, corresponding to nominal electrode areas of <1 m^2 to treat ~ 1 kg day^{-1} of PFAS. However, these values represent optimistic lower bounds. In practice, additional losses (e.g., reduced faradaic efficiency at higher current densities, cell voltage, mass transfer, and electrode aging) will lower the effective throughput, likely requiring larger electrode areas and multistack reactor configurations.

Scheme 1. Reaction Scheme for PFOA Degradation on BDD[a]

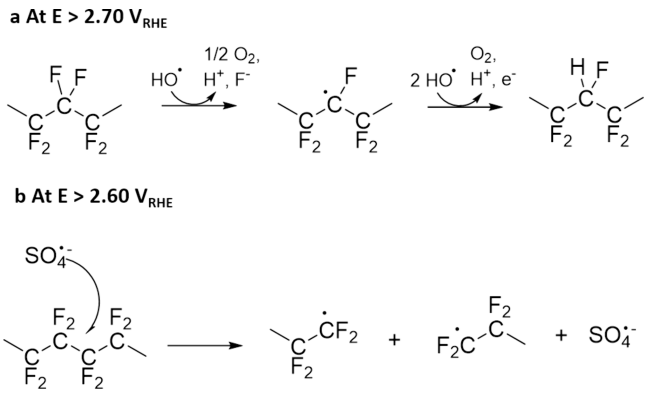

[a](a) At potentials ≥ 2.70 V_{RHE}, hydroxyl radicals form (eq 2), causing C−F cleavage and fluoride release. This reaction results into a (partially) hydrogenated carbon backbone. (b) At potentials ≥ 2.60 V_{RHE}, sulfate radicals form (eq 3-6), promoting the fragmentation of PFOA to form short-chain PFCAs. The sulfate radical eventually transforms into sulfate.[36]

https://doi.org/10.1021/acsenergylett.6c00597
ACS Energy Lett. XXXX, XXX, XXX−XXX

LITERATURE COMPARISON

Taken together, the results support an electrolyte-dependent degradation mechanism for PFOA. Hydroxyl radicals induce C−F bond cleavage along the perfluoroalkyl chain, resulting in fluoride release while preserving the carbon backbone (Scheme 1a, Figure 2). The resulting defluorinated chain is subsequently (partially) hydrogenated, as indicated by ^{1}H and ^{19}F NMR spectroscopy (Figure 3c,d). In contrast, sulfate radicals promote C−C bond scission along the perfluoroalkyl chain, leading to the formation of short-chain PFCAs (Scheme 1b). In comparison with literature, our work shows that PFOA degradation rates in perchlorate and sulfate electrolytes were comparable, which is in contrast to previous studies which proposed enhanced PFOA degradation through $SO_4^{\bullet-}$ compared to HO$^{\bullet}$ radicals.[11,38] This discrepancy can be explained by differences in solution pH: these studies were conducted at near-neutral pH, where HO$^{\bullet}$ radicals have a shorter lifetime[39] and hence are less effective by the virtue of a lower steady-state concentration available to attack PFOA. Furthermore, bicarbonate species forming from dissolved CO_2, which are present at higher concentrations at neutral than acidic pH, may scavenge HO$^{\bullet}$ radicals,[40,41] thereby suppressing HO$^{\bullet}$-driven pathways and favoring $SO_4^{\bullet-}$-driven PFOA decomposition. Through experimentation in acidic pH, our work instead shows that HO$^{\bullet}$ remains highly reactive, explaining the similar degradation rates of the parent compound PFOA in both electrolytes. As discussed in the introduction, prior studies[11,38] have focused on parent PFOA decay, without distinguishing whether HO$^{\bullet}$ or $SO_4^{\bullet-}$ radical-driven pathways lead to carbon−carbon bond cleavage or mainly to defluorination of an otherwise intact carbon backbone. In contrast, our study provides product-resolved evidence of the reaction mechanism. The closed fluorine balance demonstrates the differences in product distribution for perchlorate and sulfate electrolytes, while the unclosed carbon balance shows the loss of carbon through the mineralization of the carboxyl group. Furthermore, measuring the fluoride evolution with and without the presence of radical scavengers demonstrates the critical role of HO$^{\bullet}$ radicals in defluorination. Postelectrolysis NMR measurements, which indicate protonation of the carbon framework following defluorination, support the conclusion that HO$^{\bullet}$ radicals govern C−F bond cleavage and defluorination, whereas $SO_4^{\bullet-}$ selectively drives carbon−carbon fragmentation to short-chain PFCAs. While first-order kinetics have also been reported in prior studies,[11] it is important to consider that the observed kinetic behavior may, in part, reflect mass-transfer effects inherent to the batch configuration. Although estimates suggest that the system operates below the mass-transfer-limited regime (Supporting Information), transport limitations cannot be fully excluded under the present conditions. However, as all experiments were conducted under identical hydrodynamic conditions (stirring rate, cell geometry), any potential mass-transfer effects are expected to be comparable across electrolytes and therefore do not affect the observed differences in reaction pathways and product distributions.

IMPLICATIONS FOR ELECTROLYTE DESIGN AND STUDY LIMITATIONS

The mechanistic insights in this work suggest electrolyte design should be tuned to maximize defluorination efficiency rather than the breakdown of PFAS into shorter components. As the PFAS hazard is fundamentally tied to fluorine retention and C−F bond stability,[47] electrolytes that preferentially sustain HO$^{\bullet}$-driven defluorination can improve overall system efficiency by pushing treatment toward fluoride release rather than accumulating short-chain PFAS byproducts. Note further that the conclusions in this work remain constrained by (i) the need to generalize across structurally diverse PFAS (e.g., with different chain lengths or varying end groups),[14] which can exhibit markedly different degradation behavior, and (ii) the lack of validation under more practically relevant multi-component matrices[55] where spectator anions/cations and cocontaminant organics may scavenge radicals and alter degradation kinetics.

This study elucidates how electrolyte composition governs the radical-mediated pathways responsible for perfluorooctanoic acid (PFOA) degradation on boron-doped diamond (BDD) electrodes. By systematically comparing perchlorate- and sulfate-based electrolytes, we demonstrate that the nature of the supporting anion fundamentally alters the oxidative environment and the resulting degradation mechanisms. Despite similar fluoride release rates and overall defluorination efficiencies in both electrolytes, markedly higher concentrations of short-chain PFCAs were detected in sulfate electrolytes, indicating a distinct radical involvement. In situ electrochemical mass spectrometry confirmed CO_2 evolution, validating that mineralization accompanies the oxidative degradation of PFOA. NMR analysis revealed the formation of partially hydrogenated fluorocarbon species in perchlorate electrolyte and short-chain PFCAs in sulfate electrolyte. Through radical scavenging experiments using tert-butanol, hydroxyl radicals were identified as the dominant species responsible for C−F bond cleavage and fluoride formation, while sulfate radicals were shown to promote the formation of short-chain PFCAs. The suppression of PFOA degradation upon hydroxyl radical scavenging in the perchlorate electrolyte, combined with continued PFCA production in the sulfate electrolyte, underscores the complementary roles of these radicals. These findings shed light on the distinct pathways free radicals can drive in PFOA degradation and pave the way toward better electrolyte design, tailoring more efficient PFAS removal.

ASSOCIATED CONTENT

Supporting Information

The Supporting Information is available free of charge at https://pubs.acs.org/doi/10.1021/acsenergylett.6c00597.

Experimental methods for PFOA degradation and analytical procedures, including electrochemical setup, fluoride quantification, LC−MS calibration and evaluation, and EC−MS measurements. Literature comparison (**Table S1**). HPLC program and MS calibration parameters (**Tables S2−S3**). Calculation of the degree of defluorination, fluoride and carbon mass balance, COOH balance (**Table S4**). **Figures S1−S12**: calibration measurements, degree of defluorination, kinetic plots, mass balance over time, control experiments, and EC−MS results (PDF)

AUTHOR INFORMATION

Corresponding Authors

Haldrian Iriawan − *Department of Materials Science and Engineering, Massachusetts Institute of Technology,*

https://doi.org/10.1021/acsenergylett.6c00597
ACS Energy Lett. XXXX, XXX, XXX−XXX

Cambridge, Massachusetts 02139, United States; orcid.org/0000-0002-2997-1180; Email: haldrian@mit.edu

Yang Shao-Horn − *Department of Chemistry, Department of Materials Science and Engineering, Department of Mechanical Engineering, and Research Laboratory of Electronics, Massachusetts Institute of Technology, Cambridge, Massachusetts 02139, United States;* orcid.org/0000-0001-8714-2121; Email: shaohorn@mit.edu

Authors

Alexander Nitsche − *Department of Chemistry, Massachusetts Institute of Technology, Cambridge, Massachusetts 02139, United States*

Xiao Wang − *Department of Chemical Engineering, Massachusetts Institute of Technology, Cambridge, Massachusetts 02139, United States;* orcid.org/0000-0003-1624-8230

Yuriy Román-Leshkov − *Department of Chemical Engineering, Massachusetts Institute of Technology, Cambridge, Massachusetts 02139, United States;* orcid.org/0000-0002-0025-4233

Complete contact information is available at: https://pubs.acs.org/10.1021/acsenergylett.6c00597

Notes

The authors declare no competing financial interest.

■ ACKNOWLEDGMENTS

A.N., Y.S.-H., and H.I. acknowledge support from the Bill & Melinda Gates Foundation through Award INV-994 064006 ("Developing Efficient Carbon and Nitrogen Feedstocks for GRAS Microbes") and MIT Climate Grand Challenge - Center for Electrification and Decarbonization of Industry (MIT-CEDI). H.I. gratefully acknowledges the financial support from the Martin Family Fellowship. X.W. would like to acknowledge support from the Society of Energy Scholars, administered by the MIT Energy Initiative, and the Postgraduate Scholarship - Doctoral, administered by the Natural Sciences and Engineering Research Council of Canada.

■ REFERENCES

(1) Podder, A.; Sadmani, A. H. M. A.; Reinhart, D.; Chang, N.-B.; Goel, R. Per and poly-fluoroalkyl substances (PFAS) as a contaminant of emerging concern in surface water: A transboundary review of their occurrences and toxicity effects. *J. Hazard. Mater.* **2021**, *419*, 126361.

(2) Xiao, F. Emerging poly- and perfluoroalkyl substances in the aquatic environment: A review of current literature. *Water Res.* **2017**, *124*, 482−495.

(3) Houde, M.; De Silva, A. O.; Muir, D. C. G.; Letcher, R. J. Monitoring of Perfluorinated Compounds in Aquatic Biota: An Updated Review. *Environ. Sci. Technol.* **2011**, *45*, 7962−7973.

(4) Wee, S. Y.; Aris, A. Z. Revisiting the "forever chemicals", PFOA and PFOS exposure in drinking water. *NPJ. Clean Water* **2023**, *6*, 57.

(5) Hansen, K. J.; Clemen, L. A.; Ellefson, M. E.; Johnson, H. O. Compound-specific, quantitative characterization of organic fluorochemicals in biological matrices. *Environ. Sci. Technol.* **2001**, *35*, 766.

(6) Fenton, S. E.; et al. Per- and Polyfluoroalkyl Substance Toxicity and Human Health Review: Current State of Knowledge and Strategies for Informing Future Research. *Environ. Toxicol. Chem.* **2020**, *40*, 606−630.

(7) Saleh, N. B. Removal of poly- and per-fluoroalkyl substances from aqueous systems by nano-enabled water treatment strategies. *Environ. Sci. (Camb).* **2019**, *5*, 198.

(8) Liu, J. Reductive Defluorination of Branched Per- and Polyfluoroalkyl Substances with Cobalt Complex Catalysts. *Environ. Sci. Technol. Lett.* **2018**, *5*, 289.

(9) Zhuo, Q.; Deng, S.; Yang, B.; Huang, J.; Yu, G. Efficient electrochemical oxidation of perfluorooctanoate using a Ti/SnO2-Sb-Bi anode. *Environ. Sci. Technol.* **2011**, *45*, 2973−2979.

(10) Liu, Y. Enhanced Perfluorooctanoic Acid Degradation by Electrochemical Activation of Sulfate Solution on B/N Codoped Diamond. *Environ. Sci. Technol.* **2019**, *53*, 5195.

(11) Samuel, M. S. Enhanced perfluorooctanoic acid (PFOA) degradation by electrochemical activation of peroxydisulfate (PDS) during electrooxidation for water treatment. *Sci. Total Environ.* **2024**, *942*, 173736.

(12) Lin, H.; Niu, J.; Ding, S.; Zhang, L. Electrochemical degradation of perfluorooctanoic acid (PFOA) by Ti/SnO2-Sb, Ti/SnO2-Sb/PbO2 and Ti/SnO2-Sb/MnO2 anodes. *Water Res.* **2012**, *46*, 2281.

(13) Zhuo, Q. Degradation of perfluorinated compounds on a boron-doped diamond electrode. *Electrochim. Acta* **2012**, *77*, 17.

(14) Bentel, M. J. Defluorination of Per- and Polyfluoroalkyl Substances (PFASs) with Hydrated Electrons: Structural Dependence and Implications to PFAS Remediation and Management. *Environ. Sci. Technol.* **2019**, *53*, 3718.

(15) Sahu, S. P.; et al. Rapid Degradation and Mineralization of Perfluorooctanoic Acid by a New Petitjeanite Bi3O(OH)(PO4)2 Microparticle Ultraviolet Photocatalyst. *Environ. Sci. Technol. Lett.* **2018**, *5*, 533−538.

(16) Li, X.; et al. Efficient photocatalytic decomposition of perfluorooctanoic acid by indium oxide and its mechanism. *Environ. Sci. Technol.* **2012**, *46*, 5528−5534.

(17) Vecitis, C. D.; et al. Sonochemical degradation of perfluorooctanesulfonate in aqueous film-forming foams. *Environ. Sci. Technol.* **2010**, *44*, 432−438.

(18) Moriwaki, H.; et al. Sonochemical decomposition of perfluorooctane sulfonate and perfluorooctanoic acid. *Environ. Sci. Technol.* **2005**, *39*, 3388−3392.

(19) Stratton, G. R.; et al. Plasma-Based Water Treatment: Efficient Transformation of Perfluoroalkyl Substances in Prepared Solutions and Contaminated Groundwater. *Environ. Sci. Technol.* **2017**, *51*, 1643−1648.

(20) Mitchell, S. M.; Ahmad, M.; Teel, A. L.; Watts, R. J. Degradation of Perfluorooctanoic Acid by Reactive Species Generated through Catalyzed H 2 O 2 Propagation Reactions. *Environ. Sci. Technol. Lett.* **2014**, *1*, 117−121.

(21) Gebreab, K. Y. Comparative toxicometabolomics of perfluorooctanoic acid (PFOA) and next-generation perfluoroalkyl substances. *Environ. Pollut.* **2020**, *265*, 114928.

(22) Wang, Y.; Xu, H.; Li, R. Enhanced electrooxidation of per and polyfluoroalkyl substances on Boron doped diamond anode in the presence of vacuum ultraviolet irradiation. *Sci. Rep. 15*, (**2025**). DOI: 10.1038/s41598-025-07386-8

(23) Uner, N. B.; Baldaguez Medina, P.; Dinari, J. L.; Su, X.; Sankaran, R. M. Rate, Efficiency, and Mechanisms of Electrochemical Perfluorooctanoic Acid Degradation with Boron-Doped Diamond and Plasma Electrodes. *Langmuir* **2022**, *38*, 8975.

(24) Nienhauser, A. B. Boron-doped diamond electrodes degrade short- and long-chain per- and polyfluorinated alkyl substances in real industrial wastewaters. *J. Environ. Chem. Eng.* **2022**, *10*, 107192.

(25) Ochiai, T. Efficient electrochemical decomposition of perfluorocarboxylic acids by the use of a boron-doped diamond electrode. *Diam. Relat. Mater.* **2011**, *20*, 64.

(26) Uwayezu, J. N. Electrochemical degradation of per- and polyfluoroalkyl substances using boron-doped diamond electrodes. *J. Environ. Manage.* **2021**, *290*, 112573.

(27) Smith, S. J. Electrochemical Oxidation for Treatment of PFAS in Contaminated Water and Fractionated Foam—A Pilot-Scale Study. *ACS EST Water* **2023**, *3*, 1201.
(28) Blotevogel, J.; Thagard, S. M.; Mahendra, S. Scaling up water treatment technologies for PFAS destruction: current status and potential for fit-for-purpose application. *Curr. Opin. Chem. Eng.* **2023**, *41*, 100944.
(29) Noori, M. T.; Gupta, P.; Hellgardt, K.; Min, B. Per- and polyfluoroalkyl substances (PFAS): An emerging environmental challenge and (microbial)bioelectrochemical treatment strategies. *Curr. Opin. Environ. Sci. Health* **2025**, *43*, 100588.
(30) Ganiyu, S. O.; Martínez-Huitle, C. A.; Oturan, M. A. Electrochemical advanced oxidation processes for wastewater treatment: Advances in formation and detection of reactive species and mechanisms. *Curr. Opin. Electrochem.* **2021**, *27*, 100678.
(31) Feijoo, S.; Baluchová, S.; Kamali, M.; Buijnsters, J. G.; Dewil, R. A combined experimental and computational approach to unravel degradation mechanisms in electrochemical wastewater treatment. *Environ. Sci. (Camb).* **2024**, *10*, 652.
(32) Pei, S.; You, S.; Ma, J.; Chen, X.; Ren, N. Electron Spin Resonance Evidence for Electro-generated Hydroxyl Radicals. *Environ. Sci. Technol.* **2020**, *54*, 13333.
(33) Zhong, S. Overlooked Impacts of Alcohols in Electro-H2O2 and Fenton Chemistry. *Environ. Sci. Technol.* **2024**, *58*, 14585.
(34) Mirabediny, M.; et al. Effective PFAS degradation by electrochemical oxidation methods-recent progress and requirement. *Chemosphere* **2023**, *321*, 138109.
(35) Fang, J.; et al. Treatment of per- and polyfluoroalkyl substances (PFAS): A review of transformation technologies and mechanisms. *J. Environ. Chem. Eng.* **2024**, *12*, 111833.
(36) Lutze, H. V.; Brekenfeld, J.; Naumov, S.; von Sonntag, C.; Schmidt, T. C. Degradation of perfluorinated compounds by sulfate radicals − New mechanistic aspects and economical considerations. *Water Res.* **2018**, *129*, 509−519.
(37) Niu, J.; Li, Y.; Shang, E.; Xu, Z.; Liu, J. Electrochemical oxidation of perfluorinated compounds in water. *Chemosphere* **2016**, *146*, 526−538.
(38) Asadi Zeidabadi, F.; Banayan Esfahani, E.; McBeath, S. T.; Dubrawski, K. L.; Mohseni, M. Electrochemical degradation of PFOA and its common alternatives: Assessment of key parameters, roles of active species, and transformation pathway. *Chemosphere* **2023**, *315*, 137743.
(39) Tampieri, F.; Ginebra, M.-P.; Canal, C. Quantification of plasma-produced hydroxyl radicals in solution and their dependence on the pH. *Anal. Chem.* **2021**, *93*, 3666.
(40) Wu, C.; Linden, K. G. Phototransformation of selected organophosphorus pesticides: Roles of hydroxyl and carbonate radicals. *Water Res.* **2010**, *44*, 3585.
(41) Buxton, G. V.; Elliot, A. J. Rate constant for reaction of hydroxyl radicals with bicarbonate ions. *International Journal of Radiation Applications and Instrumentation. Part 27*, (**1986**).241
(42) Kutsuna, S.; Hori, H. Rate constants for aqueous-phase reactions of SO4- with C2F5C(O)O- and C3F 7C(O)O- at 298 K. *Int. J. Chem. Kinet.* **2007**, *39*, 276.
(43) Maruthamuthu, P.; Padmaja, S.; Huie, R. E. Rate constants for some reactions of free radicals with haloacetates in aqueous solution. *Int. J. Chem. Kinet.* **1995**, *27*, 605.
(44) Li, D. et al.. The Determination of Trace Per-and Polyfluoroalkyl Substances and Their Precursors Migrated into Food Simulants from Food Contact Materials by LC-MS/MS and GC-MS/MS. *LCGC NORTH AMERICA* vol. *37* (**2019**).7
(45) Hori, H. Decomposition of environmentally persistent perfluorooctanoic acid in water by photochemical approaches. *Environ. Sci. Technol.* **2004**, *38* (22), 6118.
(46) Shi, H.; et al. Degraation of Perfluorooctanesulfonate by Reactive Electrochemical Membrane Compose of Magnéli Phase Titanium Suboxie. *Environ. Sci. Technol.* **2019**, *53*, 14528−14537.
(47) Gar Alalm, M.; Boffito, D. C. Mechanisms and pathways of PFAS degradation by advanced oxidation and reduction processes: A critical review. *Chemical Engineering Journal* **2022**, *450*, 138352.
(48) Zhang, B. T.; Zhang, Y.; Teng, Y.; Fan, M. Sulfate radical and its application in decontamination technologies. *Crit. Rev. Environ. Sci. Technol.* **2015**, *45*, 1756−1800.
(49) Heerah, K.; Waclawek, S.; Konzuk, J.; Longstaffe, J. G. Benchtop 19F NMR spectroscopy as a practical tool for testing of remedial technologies for the degradation of perfluorooctanoic acid, a persistent organic pollutant. *Magn. Reson. Chem.* **2020**, *58*, 1160.
(50) Camdzic, D.; Dickman, R. A.; Aga, D. S. Total and class-specific analysis of per- and polyfluoroalkyl substances in environmental samples using nuclear magnetic resonance spectroscopy. *Journal of Hazardous Materials Letters* **2021**, *2*, 100023.
(51) Guerra-Rodríguez, S.; Rodríguez, E.; Singh, D.; Rodríguez-Chueca, J. Assessment of Sulfate Radical-Based Advanced Oxidation Processes for Water and Wastewater Treatment: A Review. *Water (Basel).* **2018**, *10*, 1828.
(52) Hossain, R.; Dickinson, J. J.; Apblett, A.; Materer, N. F. Detection of Hydrogen Peroxide in Liquid and Vapors Using Titanium(IV)-Based Test Strips and Low-Cost Hardware. *Sensors* **2022**, *22*, 6635.
(53) Urbanas, D.; Baltrėnaitė-Gedienė, E. A critical review of the methods being proposed to solve the PFAS problem in drinking water: Are they practically applicable in real world? *Emerg. Contam.* **2025**, *11*, 100563.
(54) Yanagida, A.; Webb, E.; Harris, C. E.; Christenson, M.; Comfort, S. Using Electrochemical Oxidation to Remove PFAS in Simulated Investigation-Derived Waste (IDW): Laboratory and Pilot-Scale Experiments. *Water (Switzerland)* **2022**, *14*, 2708.
(55) Awoyemi, O. S.; Munyeza, C. F.; Sharma, A.; Naidu, R.; Fang, C. Ultrasonication degradation of per- and polyfluoroalkyl substances (PFAS) in synthetic environmental samples: Impact of ionic composition and water chemistry. *Journal of Water Process Engineering* **2025**, *77*, 108376.

https://doi.org/10.1021/acsenergylett.6c00597
ACS Energy Lett. XXXX, XXX, XXX−XXX